OPTIMIZATION OF PERMANENT MAGNET ASSISTED SYNCHRONOUS RELUCTANCE MOTOR (PMA-SYNRM) EMPLOYING HIGH-STRENGTH ROTOR LAMINATION (NIMARK 300 ALLOY)

BY

ALEJANDRO LONGARES CONEJO

THESIS

Submitted in partial fulfillment of the requirements
for the degree of Bachelor of Science in Electrical Engineering
in the Graduate College of the
University of Illinois at Urbana-Champaign, 2020

Urbana, Illinois

Adviser:

Kiruba Sivasubramaniam Haran

ABSTRACT

Energy storage improvement for electric mobility has become trending topic in I+D, whereas electric machinery performance has been left aside due to its enormous technology advances during the last two decades, even though it has still a wide range of improvement. This thesis investigates the potential of improved performance of a Permanent Magnet Assisted Synchronous Reluctance Motor (PMa-SynRM) considering an unusual material for its lamination. The significant feature of this proposed material is its great mechanical properties which enable rotor lamination designs better suited for high speed synchronous reluctance motors. However, the material is relatively poor in magnetic capability. Hence, a detailed electromagnetic and mechanical analysis has to be performed to understand the net benefit of employing this material. Three different rotors with same shaft and outside dimensions have been designed to test electromagnetic efficiency and mechanical resistance by the finite-element method. Torque, total reactance, flux density and magnetic field can be evaluated to conclude if this material with its respective modifications provides a better overall performance as well as higher power density to improve electric mobility through electric traction performance.

To my parents, for their persistence in enforcing me to follow my passion and to the people who influenced me to study this field.

ACKNOWLEDGMENTS

This research would not have been possible without the resources offered by the Electrical and Computer Engineering (ECE) department of the University of Illinois. Therefore, I want to thank all the professionals who work in the ECE building, specially Prof. Haran, my advisor for this thesis and Peter Xiao, my co-worker during my research.

Thank you.

TABLE OF CONTENTS

LIST OF FIGURES

CHAPTER 1

INTRODUCTION

High Efficiency remanufacturing (HER) of electric machines is a topic that has been developed through the past years by many universities and investigation centers to bring electromagnetic machines efficiency to its maximum [2]. However, many companies are having difficulty financing the newest technology in electric traction due to its high production cost. The fact that a profitable company like Tesla uses the primitive induction motor technology for their famous high performance electric vehicles [3], is a proof that the newest technology for high electric power mobility is no viable option for any company whose priority is financial profit.

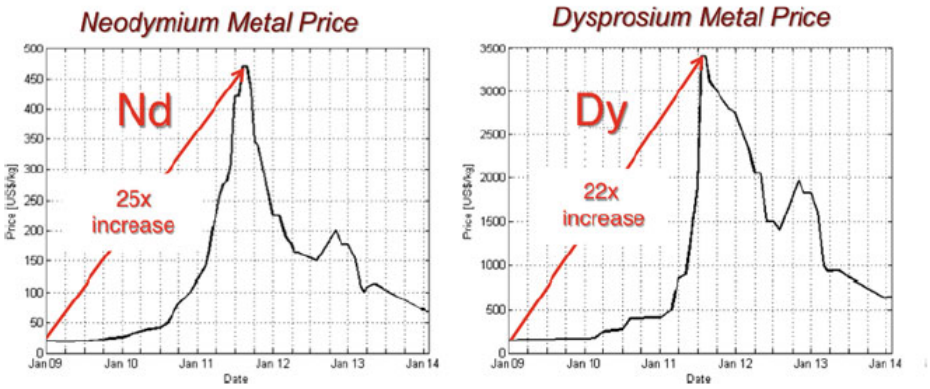

Figure 1.1: Price volatility of rare magnets

The permanent magnet synchronous machine (PMSM) is a good example to explain the mentioned issue. The performance of this machine during the last decade has been extremely positive and has meant a big advance in electric mobility. Its excellent efficiency in high power applications, the power/torque capability and its great dynamic response during high speed functions have led companies like Toyota to use this technology to power one of their most profitable hybrid vehicle (HV) models (Toyota Camry, 2007).

Fields like aviation, which require even more powerful mobility, have started to bet on a possible future where planes are only powered by turboelectric propulsion. However, the materials that are used to manufacture these types of machines, such as neodymium and dysprosium (rare magnets), are limited in our planet. Thus, the price volatility is extremely high. In Fig. 1.1, we can see that the prices of these two materials increased 25x in less than three years [1]. This increase produced an unstable market and therefore an unexpected issue for those companies who depend on these materials. In addition, there is clearly a dominant country in the rare-magnet production, which is China. Figure 1.2 shows the production in metric tons (MT) during 2018 [4]. China produced hundred thousand metric tons more than Australia, which is the second largest producing country. This leads unfortunately to a high dependence on rare-magnet importation from China. This situation is comparable to the petroleum dependence on Middle Eastern countries. The only difference is that countries like USA cannot compete with China's production, since we are talking about thousands of tons of difference whereas in the oil production, there are many countries that are self-sufficient. Besides the macroeconomic concerns, there is also a big mechanical issue, which is the demagnetization of rare magnets in high power applications due to heating [5]. The cohesive force tends to decrease drastically while the machine is running at high temperatures. Hence, the hard-magnet evolves to a soft-magnet and the high torque capability of the machine is lost. This issue is very problematic for PMSM since the great mechanical properties are lost over time.

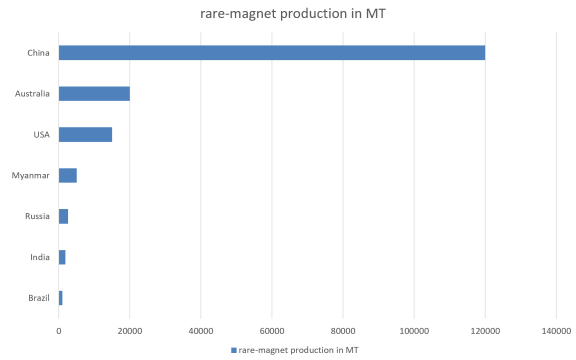

Figure 1.2: Rare magnet production in metric tons

The synchronous reluctance machine (SynRM) has been very popular for electric power applications due to its reliability and low-cost manufacture when weight and size of the motor were not a priority [6]. However, in electric traction, both of the mentioned magnitudes have a high impact on power density, which is the main factor for motor efficiency.
Therefore, we need to investigate other machines that could be used to perform the same power output with the same efficiency ratio for high frequency and power applications, or at least similar. Due to the issues mentioned above, the permanent magnet assisted synchronous reluctance machine (PMa-SynRM) has been a reasonable substitute for PMSM applications. Although it has not the same power and dynamic capabilities, it reduces considerably the cost of manufacture since rare magnets are replaced by magnet ferrite bars. The positive feature of this machine is the potential use of the reluctance torque by playing with the q-d axis inductance. The theoretical idea of this motor will be explained later on. However, to reach the torque capability and efficiency of a PMSM, the PMa-SynRM needs to be improved by its design and material selection to create a machine capable of meeting the expectations of powering seamlessly an EV.

This thesis investigates the possible power and efficiency improvement of a PMa-SynRM by using a uncommon material for rotor lamination called NiMark 300 Alloy. It is a high temperature alloy capable of attaining yield strengths in excess of 1862 MPa through simple, low temperature heat treatment. Its mechanical properties make this material an excellent candidate for rotor lamination to reduce the core bridges as much as possible, which could lead to a possible torque performance. The main idea of this research is to manufacture three rotors with different features to compare torque and efficiency and observe if this used material could be cost-effective. The design used for our first two rotors has been taken from a previous project created by the "Haran research group". The only difference between these two rotors is the lamination material. Unlike the first two, the last rotor has an improved design regarding its rotor reluctance using the provided steel alloy. Once the designs were finished, including shaft and ferrite bars placement, the rotors should have been manufactured by the end of the spring semester. However, due to the pandemic, we were not able to continue with our manufacturing plans. As a result, we decided to focus more on the electromagnetic

properties of our lamination and simulate the obtained design through FEA in Inventor with an advanced software such as MotorCad. We were afraid that our second lamination would not be able to hold the real tensions at which our motor was going to be exposed. Finally, we found a design that, even though it was not as profitable as expected, it increased the power efficiency compared to the first rotor and resisted stress values up to 90 % of its yield strength at 14000 rpm (rated speed). Simulating our final design in Inventor, we observed that the ferrite bars placed between the air gaps of our lamination considerably reduced the stress resistance of the iron bridges. However, considering the fact that the change of material finally improved the machine performance, we can conclude that the final design is not only capable of fulfill all the requirements for an efficient power machine, but is also cost-effective for possible mass-production.

CHAPTER 2

LITERATURE RESEARCH

2.1 PMa-SynRM

The PMa-SynRM is an adjusted combination of the PMSM and SynRM. This machine modifies the reluctance of the rotor as well as the permanent magnets to produce an interesting average power output. The most common design for a 4-Pole machine is shown in Fig. 2.1 .

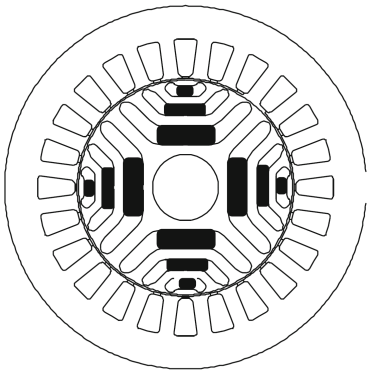

Figure 2.1: PMa-SynRM [1]

The most important feature of this machine is the use of magnetized ferrite bars instead of rare magnets. The additional power created by the magnetically-salient rotor structure allows the machine to not only rely on the cohesive force of the magnets to produce torque, which gives the opportunity to use another non-rare material with less than a half of the cohesive force of neodymium for half the price, like magnetized ferrite bars [7]. This reduces considerably the cost of production of our machine.

The use of ferrite ceramic permanent magnets became commercially available in the 1960s as a lower-cost alternative to rare magnets. The low cost of ferrite magnets combined with their other attractive features, including excellent corrosion resistance, has led to their tremendous commercial success. In fact, ceramic magnets today account for over 75 % of all magnet consumption in the world on the basis of shipped magnet mass.[1]
We define the PMa-SynRM as an adjusted combination due to the modification of the use of permanent magnets, as we explain in the next section.

2.1.1 Q-d axis flux distribution

In the PMa-SynRM, our d-axis represents the maximum flux density flow for a specific pole of the machine, whereas the q-axis represents the minimum. I shall remind that the q and d-axis are phase-shifted up to 90 electrical degrees [8].
In the case of our example in Fig. 2.2, our motor has a total of 8 poles, which means that if we want to convert our electrical degrees in mechanical, we need to use the formula

$$Degrees_{mec} = \frac{2}{P} \times Degrees_{elec} \tag{2.1}$$

therefore, we obtain a total of 22.5 degrees, as shown in Fig. 2.2. If we represent the q-d-axes of a PMSM, we observe that the maximum flux density flow of the machine, represented by the d-axis, does not match with the representation of the d-axis shown in our PMa-SynRM design. Whereas in the PMSM the d-axis is aligned with the permanent magnets of the machine, in the PMa-SynRM the d-axis is aligned with the core paths drawn in the rotor lamination and the ferrite bars are aligned with the minimum flux density flowing through the machine. The scientific explanation for this phenomenon is that the magnets are not being used for the same purpose. In the PMa-SynRM, their main goal is to oppose the magnetic flux created in the q-axis by the rotor inductance in this direction and as a result increase the torque capability of the machine. Figure 2.2 illustrates the main idea of this concept. In the PMSM, the permanent magnets are creating the entire magnetic flux through the machine and therefore it is the only source that this machine has

to create magnetic flux, since it does not have a magnetically-salient rotor structure to produce power. There are infinite solutions for a PMa-SynRM due to their multiple design possibilities to combine permanent magnets and magnetic-saliency to produce torque. In fact, there has been a research about a possible design that could be revolutionary for the electric machinery [9]. In this thesis we will work with the most conventional design which has been introduced earlier. To find the optimum design, there are some basic leads we can follow that will always improve our machine.

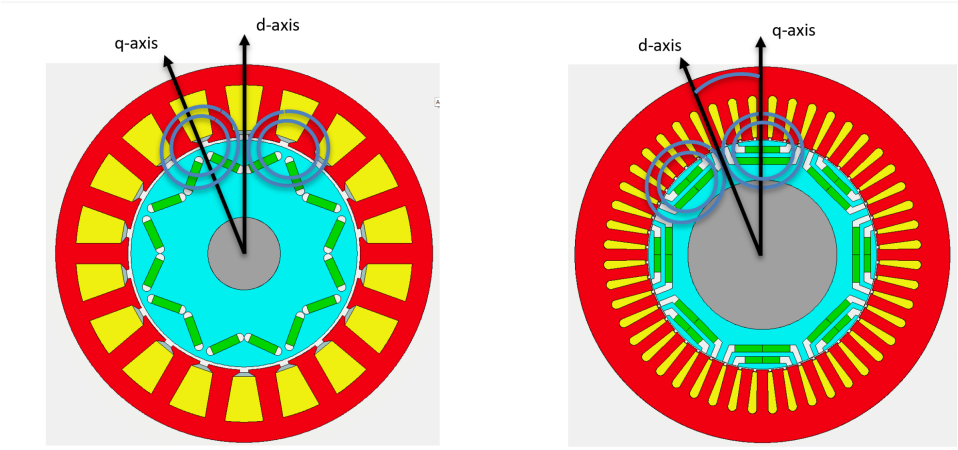

Figure 2.2: Q-d axis representation of IPMSM and PMa-SynRM

Regarding the magnetic term of our power, the torque capability depends mainly on the cohesive force of the magnet and the amount of material. This is why rare magnets are more efficient than magnetized ferrite.
In the case of the reluctance term of the torque, we always look for a magnitude called *salient-ratio*, which is defined as

$$\varepsilon = \frac{L_d}{L_q} \tag{2.2}$$

L_d is the inductance value of the maximized flux density axis, whereas L_q is the inductance of the q-axis aligned with the minimum flux density flow due to the low magnetic permeability of the permanent magnets and the air. To obtain maximum efficiency and maximum torque capability, we will always try to make the saliency ratio of our machine as high as possible.[1]

2.1.2 Torque definition through mathematical deduction

To understand the purpose of the ferrite magnets and the saliency ratio, we have taken the liberty to represent the phasor diagrams of a SRM and a PMa-SynRM. Both diagrams represent the main magnitudes of their respective machines. Since our axes are represented by d and q, we need to define our machine magnitudes referred to the new 2D coordinate system. Hence, all magnitudes will have a q and d-axis value, as shown in Fig. 2.3 (e.g. $\vec{I} \rightarrow \vec{I_d}; \vec{I_q}$). Now we are going to define the universal equation for power:

$$P = Re\{\vec{V} \times \vec{I^*}\} \tag{2.3}$$

$$P = \vec{V} \times \vec{I} \times \cos\phi \tag{2.4}$$

where ϕ is the phase angle between both vector magnitudes[1]. Like we said in the introduction, the drawback of the SynRM is its low power factor. If we look at ϕ in the SynRM phasor representation, we can appreciate that the angle is considerably big for an electric machine. The main reason is the total flux linkage [Λ] created by the magnetically-salient rotor structure. Our voltage phasor $\vec{V}$ results of multiplying Λ by jw. The saliency ratio of this particular machine is not big enough to reduce ϕ to a reasonable value that could be considered as acceptable. On the other hand, comparing both phase angles ϕ (PMa-SynRM with SynRM) it is clearly visible that the PMa-SynRM has a smaller angle at equal conditions, and thus a higher power factor. The magnetized ferrite bar in the PMa-SynRM creates an additional flux linkage on the q-axis that counteracts the one created by the rotor inductance along the same axis $L_q I_q$ (Fig. 2.3).

The positive effect of this feature becomes more obvious once we look at the phasor diagram of the PMa-SynRM (Fig. 2.3). Since our total voltage $\vec{V}$ is defined as:

$$\vec{V_T} = \sum \vec{V_f} \tag{2.5}$$

where V_f represents the different voltage drops created by the different flux linkages, we need to add the voltage drop created by the magnets to our expression. This additional term brings our resultant vector closer to the armature current, since it moves from the 2^{nd} quadrant to the 1^{st}. Hence, we obtain a higher power factor.

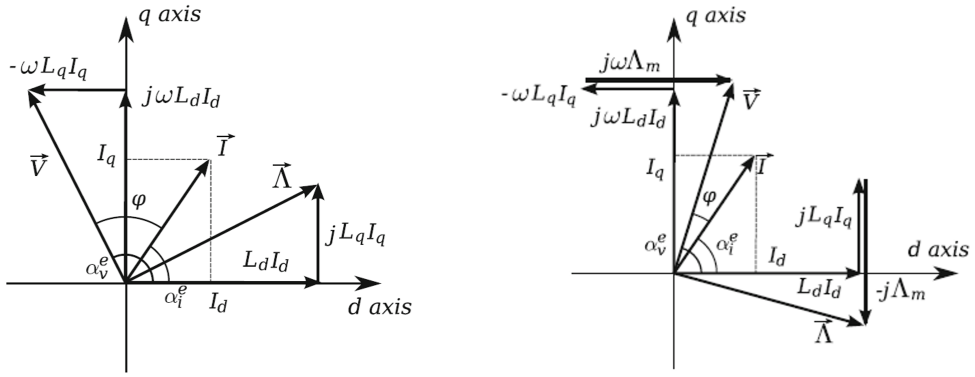

Figure 2.3: Phasor diagram of SynRM (left) and PMa-SynRM (right)

This effect is also reflected in the final Torque equation of each machine

$$\tau_{em} = \frac{3}{2} p(L_d - L_q) i_d i_q \tag{2.6}$$

$$\tau_{em} = \frac{3}{2} p(L_d - L_q) i_d i_q + \frac{3}{2} p\Lambda i_d \tag{2.7}$$

Equation 2.6 represents the electromagnetic torque produced by SynRM whereas equation 2.7 represents the same magnitude produced by a PMa-SynRM. The magnetic term in equation 2.7 is increasing the average torque of our machine, which means that its positive influence on the torque capability has been mathematically demonstrated.

2.1.3 Increasing torque capability through core bridge reduction

After we finally defined the torque equation for the machine we are going to use, we will introduce the main purpose of our idea. The main issue we encounter in the PMa-SynRM is still the inductance term in the q-axis which reduces considerably the power output of our machine and therefore its torque capability. To reduce this term, the first method we think about is the increase in the saliency ratio mentioned in 2.2.1 . However, this has been already done and it has been extremely profitable, but every material has its limits. Since the geometry of our rotor is sustained partially by small

core bridges pointing to the q-axis, it is impossible to further reduce its dimensions to reduce even more L_q, since the material with great magnetic properties we are using to produce stack our rotor lamination would not stand such high stress. The reason we want to reduce the bridges is because we want to increase the amount of air obtained in the q-axis. Due to its low magnetic permeability, the air gaps creates a higher reluctance and hence a lower inductance. Thus, we are considering using a high strength material that can stand up to 2000 MPa of yield strength to reduce considerably the size of our core bridges and hence reduce L_q, which would lead in an increase in final torque. Thus, we can define our main idea as replacing the core material of our rotor by a high strength steel alloy to increase our power output and consequently its average torque. However, there is a side effect by exchanging the materials we need to consider. Although our new material has excellent mechanical properties as we will see on section 2.2, we will lose magnetic permeability in the d-axis, which is the reason of flux density production by magnetic field excitation.

2.2 Material Properties

This thesis focuses most of its research on study the behaviour of the two selected materials, since the key of our success is in the material lamination. Therefore, we decided that the selected materials should be introduced and described in an entire section, so the reader is able to know more about its magnetic and mechanical properties and understand the reason why we are selecting these and no others. The first material we are going to describe is one of the most common materials used for rotor lamination nowadays. Secondly, we are going to describe the proposed material that should improve the efficiency and torque capability of the PMa-SynRM.

2.2.1 DI-Max HF-10X

DI-MAX HF-10X is a non-oriented electrical steel designed for use in electrical high speed motors, aircraft generators, and other rotating equipment operating at frequencies above 60 Hz due to its great magnetic properties. This type of electrical steel has a silicon level between 2 and 3.5% [10] - [11]

and has similar magnetic properties in all directions. This feature allows the magnetic flux to distribute along the core smoothly and uniform, no matter which direction the flux is currently flowing. The reason why this material is so popular for high speed motors is because of its superior permeability at high inductions.

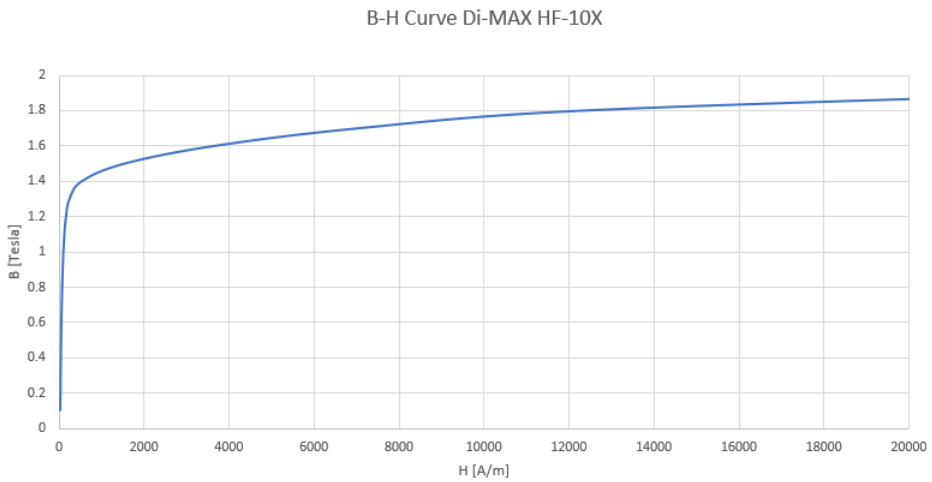

Figure 2.4: DI-MAX HF10X's B-H Curve

If we look at its B-H Curve (Fig. 2.4), we observe that the flux density along the material can reach up to almost 1.9 T at high magnetic field excitation. In addition, this material is recommended due to its low average core loss. On the other hand, the mechanical properties of this material leaves much to be desired. It can stand up to 440 MPa of yield strength and 570 MPa of tensile strength. One last feature we need to add to this material is its cold finishing plus strip annealing that provides its manufacturer, which produces a smooth surface and thus a great stacking factor. In our case, since our machine is stacked parallel to the main flux path, the magnitude we most care about is the stack tangential relative permeability, which is not highly sensitive to the stacking factor. A property that is also important to consider is the density of the material. DI-MAX HF-10X has a density of 7600 kg/m^3, which is a low value compared to other common steels.

2.2.2 NiMark 300 Alloy

NiMark 300 Alloy is a low-carbon, nickel-cobalt-molybdenum high temperature alloy member of the *maraging* steels capable of attaining yield strengths of 1862 MPa through simple, low temperature heat treatment (482 Degrees). In addition, this material has a good ductility at high strengths levels and excellent notch ductility. The material we are going to use for our research has been donated from *Carpenter Technology* to our college. After a specific heat treatment, our material can stand up to 2020 MPa of yield strength and 2038 Mpa of tensile strength. This mechanical properties makes NiMark the best fit for our new rotor design. However, like we anticipated on section 2.1.3 , the magnetic properties of this new proposed material are poor, since its magnetic permeability is small for low field excitation values. If we look at the B-H Curve, we observe that the material does not tend to saturate until 4000 A/m.

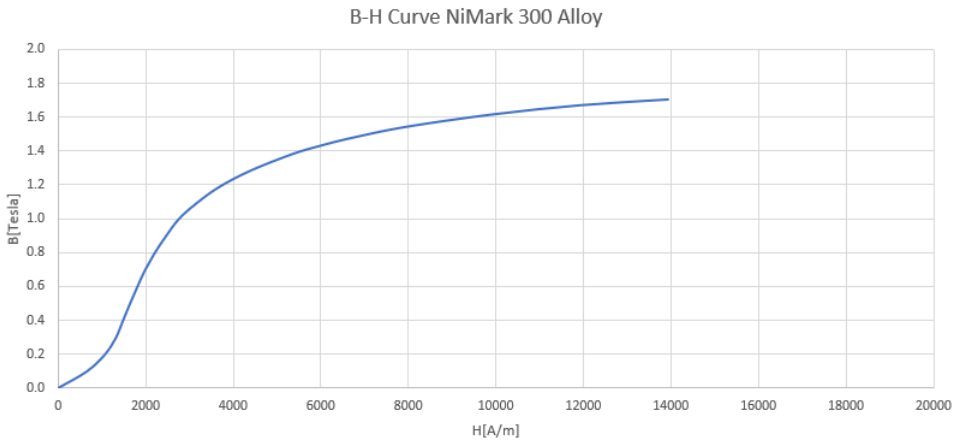

Figure 2.5: NiMark 300 Alloy's B-H Curve

2.2.3 Properties comparison

In this section, we are going to do an analysis of which are the best operating conditions to enhance the properties of our selected material. In order to achieve this, we need to look and compare both materials.
First of all we are going to look at their magnetic properties. If we have a look at their respective B-H Curves, we can observe that our new material

produce very low flux density at low magnetic field excitation compared to DI-MAX HF-10X. For 1000 A/m, The non-oriented electrical steel produces almost 8 times more flux density than the *maraging* steel (1.5 vs 0.2) due to its great magnetic permeability. However, if we observe the shape of the curve (DI-MAX), due to the fact that the material tends to saturate so fast, the amount of Teslas produced at different A/m is almost constant. As a result, the flux density produced by both material at high field excitation is very similar. If we look at our NiMark steel B-H Curve, its magnetic permeability is way lower than the electrical steel. Therefore, this material needs a great amount of A/m to achieve a value that is close to its maximum flux density (we observe a much flatten curve). High flux density at low A/m is a great advantage for many applications since the amount of power needed to achieve its maximum flux density is very low. Yet in our case, where our motor will be running to motorize high power systems, this attribute is not so important like in other applications and therefore the difference between choosing one material over the other is not that big. In conclusion to the magnetic properties, we can assume that the lose of magnetic permeability due to the material change would not have such a negative result on the final power output at high power applications.

After arguing about the magnetic properties of both materials, we are going to study their mechanical attributes. The most important magnitudes to consider are yield strength and material density. Normally we do not take tensile strength in consideration, since we do not want our machine to plasticize under any circumstances. However, our machine could operate due to a possible fault under extreme conditions, where the yield strength value could be overcome. Therefore, we always look that the difference between both magnitudes is big enough not to suffer any unfortunate accidents. In the case of mechanical properties, the only phenomenon that can vary their values is temperature, and the effect it produces to the material is similar to all type of steels. In this experiment, we consider that their mechanical properties does not vary at any operation point. If we compare the yield strength values given in (2.2.2) and (2.2.3), we observe that NiMark 300 Alloy can stand almost 5 times more stress than our common used non-oriented electrical steel without plasticize, no matter at what speed the motor is running or what magnetic field excitation the machine is suffering. This gives us the

opportunity to reduce our bridge sizes to their minimum. As we will see in our simulation results, the biggest bridge difference between the two different designs is 0.75 mm.
On the other hand, our new material has a high density compared to the steel alloy average value, whereas DI-MAX density is optimum compared with other metals [12]. This means that although we are improving our rotor mechanical strength, we are making it heavier. At the end, we will need to determine with the help of our results whether our material is cost-effective or not.

Finally, we can conclude that by changing our lamination material, we are increasing the mechanical strength of our lamination in exchange for magnetic permeability and density.

CHAPTER 3

SIMULATION

After deducing in a theoretical way what is the repercussion we are looking to accomplish by changing our material lamination, we need to ensure that we embody our idea in simulation results.

3.1 Mechanical Simulation with FEA in Inventor

First of all, we will use Inventor Professional 2020, a very powerful software tool in terms of designing 3D structures, to create our new rotor design. With the help of its stress analysis computation, we are able to design a rotor structure that stand stress values underneath the established limits. Although this CAD tool is not optimum to run complex stress analysis (there are many other tools like ANSYS that provides more powerful results), since we are only simulating a single rotor lamination part (all identical and thus enough to test only one), Inventor should be accurate enough to obtain a reliable solution. The rotor design template we are going to use was created by the "Haran Research Group". Although this design was created for a SynRM, we decided to modify the lamination to fit our ferrite bars into the air gaps and remodel it from there. Since we modified the template, not only do we have to design our new rotor for NiMark 300 Alloy, but we also need to test our modified template with DI-MAX HF-10X and see how much we can reduce its bridge size. Fig 3.4 represent the template and the remodeled design, respectively.

3.1.1 Procedure

First of all, we need to define the geometry of our prototype. If we study our initial design, we can observe that it has 8-poles in total and therefore a

recognizable circular pattern. Hence, to speed up our simulation procedure, we are reducing our simulation area to only one eighth of our lamination. Fig. 3.1 shows a graphic interpretation of the area we are simulating.

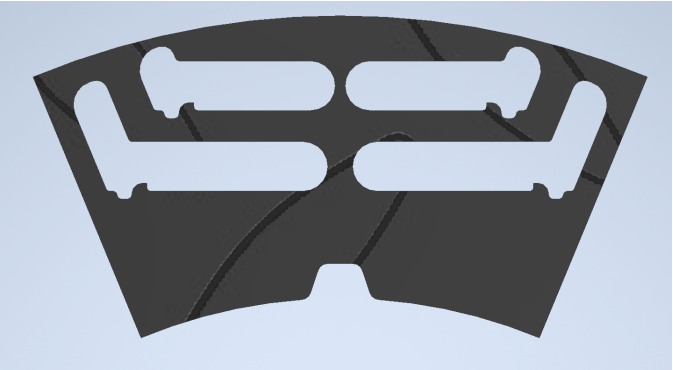

Figure 3.1: Simulation prototype of PMa-SynRM

After defining the area we are going to work with, we need to define the material properties of our prototype. Although density and yield strength are the most important magnitudes for mechanical simulations, Inventor request other mechanical attributes from the selected material such as tensile strength, Young's modulus, share modulus and its Poisson's ratio, so it can run a FEA considering elastic deformations in all possible directions. Additionally, we need to define the load our machine is suffering. In the case of our motor, the only load that it is experiencing is the centripetal force created while it is spinning. Thus, we are defining the angular speed of the machine up to its rated value, 14000 rpm. Finally, we need to set some constraints to our model, since it is rotating around a fixed point. In addition, we are defining the surfaces where we separated the pole from the main lamination as frictionless. This way we are indirectly saying to the software that this design is connected to more pieces through those surfaces. Now that we have set everything up, we can proceed to run the simulation.

The way we are going to look for our optimum design is very simple. We are going to use a brute-force method by simulating our initial design several times with different core bridges. The first simulations are not going to have the ferrite bars into consideration since it takes a lot of time changing many dimensions of two different pieces. After finding a possible optimum, we

are going to add the ferrite magnets and observe if our optimized design can stand the stress. Due to the fact that our motor could run at a higher angular speed that its rated value, it is important to leave a safety factor of min. 1.1 . The initial core bridges are defined in Fig. 3.4 (left). After simulating our piece with DI-MAX HF-10X and finding its optimum with a small amount of simulations, we are going to focus on finding the optimum for our selected steel alloy. The reason we need a small amount of simulations for this material is because the template we are using was already optimize for a very similar non-oriented electrical steel. Nevertheless, we need also to take the ferrite bars into consideration, but we can predict similar bridge sizes. In the case of our NiMark 300 Alloy, we will need more iterations to find its optimum.

3.1.2 Results

As it was expected, the bridge sizes of DI-MAX HF-10X for its optimum design are very similar to the ones defined in the template. The von mises stress distribution along the geometry is shown in Fig. 3.2 .

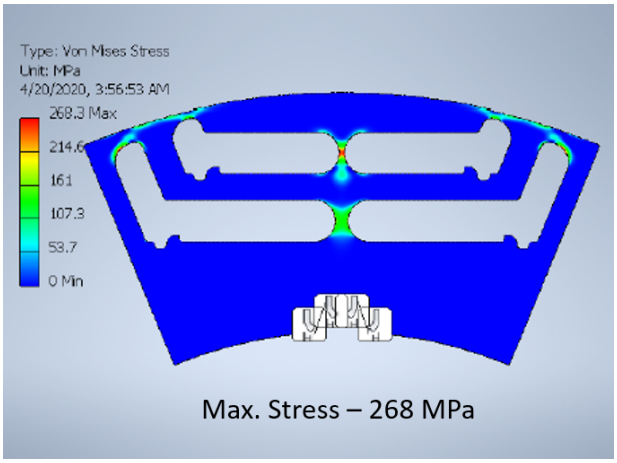

Figure 3.2: Simulation result for Di-MAX HF-10X

Our next step is finding the steel alloy optimum design. After several iterations, we found a possible optimum that could stand up to 1551 MPa, which is a good value since it fulfills by far the required power factor (1.3). However, after adding the ferrite magnets in our air gaps, the maximum

stress value increased up to 2152 MPa, which is even more than our max. tensile strength. Thus, we need to take one step back in our simulation and make our bridge reduction smaller. Finally, we found an optimum design that could meet the expectations standing at first instance up to 1332 MPa. After simulating the design including the modified ferrite bars, we obtained a max. stress of 1762 MPa leading to a power factor of 1.13 . Fig. 3.3 shows the von mises stress and power factor distribution around the simulated geometry.

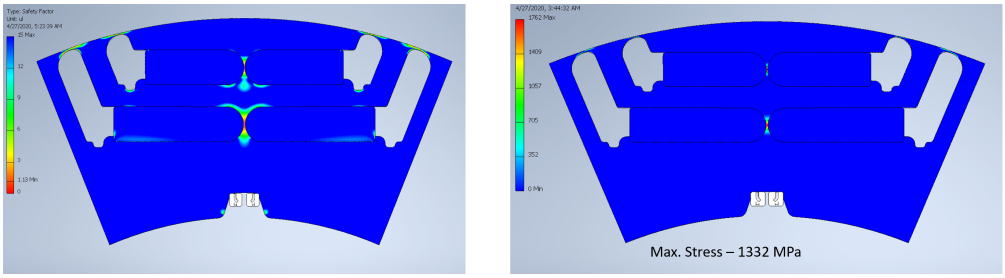

Figure 3.3: Power factor (left) and von mises stress (right) distribution

Finally, we are going to have an overview at the final optimized rotor lamination we were able to design for each material. Fig 3.4 is representing the final design for DI-MAX electrical steel and NiMark steel alloy. The difference of the bridge sizes between both designs are clearly visible. The maximum bridge reduction we are able to achieve is 0.995 mm. This is almost a millimeter of difference, which is an amount to actually take into consideration. On balance, we can conclude saying that the goal of reducing our core bridges using a high strength steel alloy has been successful. Nevertheless, we still need to ensure that this geometrical modification on our rotor lamination indeed improves the performance of our PMa-SynRM.

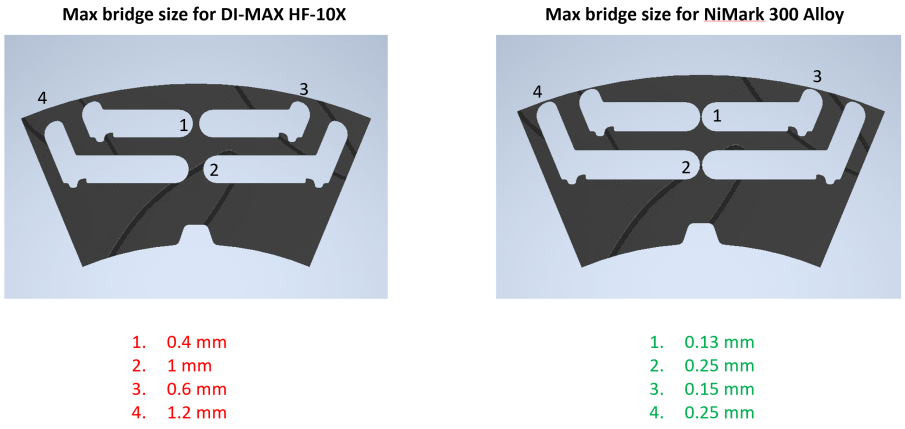

Figure 3.4: Final designs obtained for the respective materials

3.2 Electromagnetic Simulation with FEA in MotorCad

Electromagnetic simulation results are the ones that are going to determine whether our design is only counterproductive or it actually performs the power output and therefore the annealed torque capability. For this part of our simulation, we are going to use a powerful software tool called MotorCad. This CAD software belongs to ANSYS and it is specialized in electric motor simulations of any kind. The geometry transfer from Inventor to MotorCad is normally made through the creation of a .dxf file which creates a 2D representation of the lamination geometry that can be imported in MotorCad. However, with the .ipt file created in inventor, we were not able to create a .dxf file and therefore we had to recreate the rotor structure from the beginning in MotorCad. The only inconvenience we encounter as a result of this was that we could not recreate the round shape of our bridge corners. Nonetheless, since our design development had only impact on the size of the bridge and not to its shape, we can assume that this is not going to be decisive when it comes to arguing which design produces more torque. Fig. 3.5 shows the created geometry for non-oriented electrical steel (left) and NiMark 300 alloy (right).

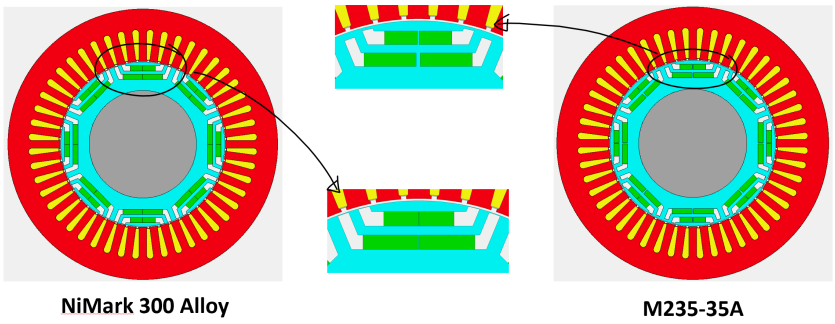

Figure 3.5: Geometry created in MotorCad for M235-35a and NiMark 300 Alloy

3.2.1 Procedure

On this simulation, we only need to run the software only once to obtain the results we are looking for, since this simulation is only executed to compare both designs and decide which motor produces more torque. We are not looking to improve our design by electromagnetic magnitudes.

First of all, we need to add our new material to the MotorCad library. Do to so, we need the B-H Curve of our steel alloy as well as its core loss curve at different frequencies. In addition, we also need to provide its volume resistivity. Although we are using DI-MAX HF-10X as the primary material for this thesis. we decided to use M235-35a in MotorCad. The reason for that is because this material is already registered in the database of our software tool, and since both materials are non-oriented electrical steels and have almost the same mechanical and electromagnetic properties, we assume that they will provide the same results and thus save a lot of time.

After we introduced both materials in their respective designs, we need to set at which armature current our motor is going to run. In this case, we decided that the rated current for our machine will be around 90 rms, which is an average value for high speed applications. To simulate the heating of our motor as well, we also set the average motor temperature to 100 degrees Celsius. All other parameters are set by default. Since both designs are going to perform under the same conditions, all parameters are valid for both designs.

3.2.2 Results

After all parameters are set and the geometries are perfectly defined, we can proceed to run our last simulation and discuss the obtained results.

Flux Density

The first magnitude we are going to discuss is the flux density created along the motor structure. Fig. 3.6 shows the obtained results for M235-35a and NiMark 300 Alloy through different colors. Red represents the max flux density created and blue its minimum. As we explained in the previous section, we are only simulating one eighth of the entire motor structure as we count with a machine defined by a circular pattern.

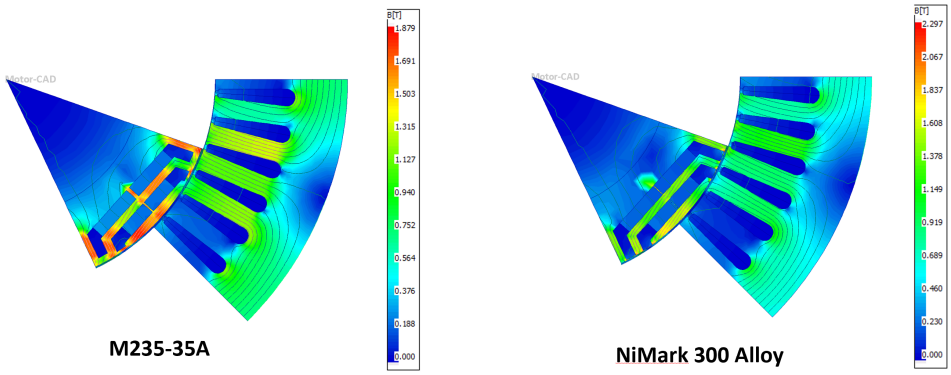

Figure 3.6: Flux density $\vec{B}$ distribution along the machine for a specific angle

In the electrical steel simulation, we can observe that the path from one d-axis to the next one is blurred with different colors and does not have a smooth continuous value among the core, since it fluctuates from 1.7 to 1.0 Tesla. This is due to the interaction of the q-axis flux, interfering with the d-axis magnitude. The width of the core bridges is too big and thus the flux aligned with them is getting stronger. This results to a bad fluency of the value that we care about, which is the q-axis flux.
In contrast, by simulating NiMark 300 Alloy we obtain a very different flux distribution along the core. The flux density between two d-axis is all uniform and maintain a constant value of 1.45 Tesla. This smoothness is provided by

the reduction of our core bridges. The q-axis flux is weakened by the loss of magnetic material and the increase of air gap aligned with it.
One observation that is not visible at first sight is that the color scale from the simulations are not equal. The maximum flux density in the M235-35a simulation is 1.8 T whereas for our NiMark the maximum flux density scaled is 2.3, although it does not arrive to this amount in any visible point in our motor.

Torque capability

Torque capability is the reason we are doing this research, since it is the main factor we are trying to improve. Thus, our goal will be accomplished if our new selected material gives a higher torque than the previous design under same conditions.

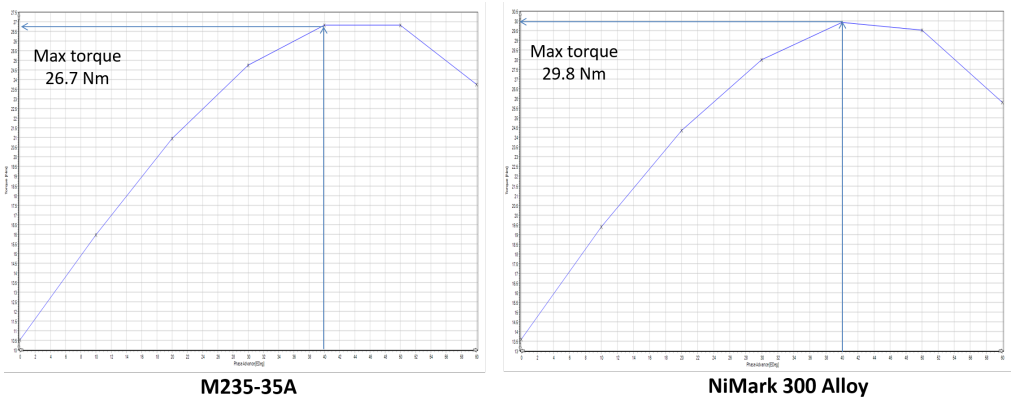

Figure 3.7: Torque capability depending on phase angle

The results obtain for this section are shown in graphs where the average torque from the machine is given at a specific phase angle. Among other values, we need to focus on the maximum torque that our machines are capable to provide. In the case of our non-oriented steel, the maximum torque is around 26.7 Nm, which is quite smaller than the one obtained with our new design (around 3 Nm). Therefore, we can now verify that our new design indeed improved the PMa-SynRM performance.

Phasor Diagram

Although this is normally not taken into consideration, in this case it is interesting to observe how the two different (by MotorCad generated) phasor diagrams look like. Fig. 3.8 is showing the phasor diagram for M235-35a (left) and NiMark 300 Alloy (right). The most important observation we did after studying these two diagrams was the improvement of the generated back emf of our ferrite magnets in our selected material due to the core bridge reduction. This magnitude is represented in the q-d axis system as the arrow that starts from the zero coordinate and is pointing upwards. The flux linkage improvement is even greater than the reduction of our flux linkage created by the q-axis inductance, which is something we did not expect. However, it has some positive impact on the overall performance. In fact, we might even say that the improved back emf is what finally allowed our new material to obtain a better performance. In addition, we can also observe the angle reduction from one model to another and thus the increase of the power factor of the machine, as we predicted in (2.1.3) .

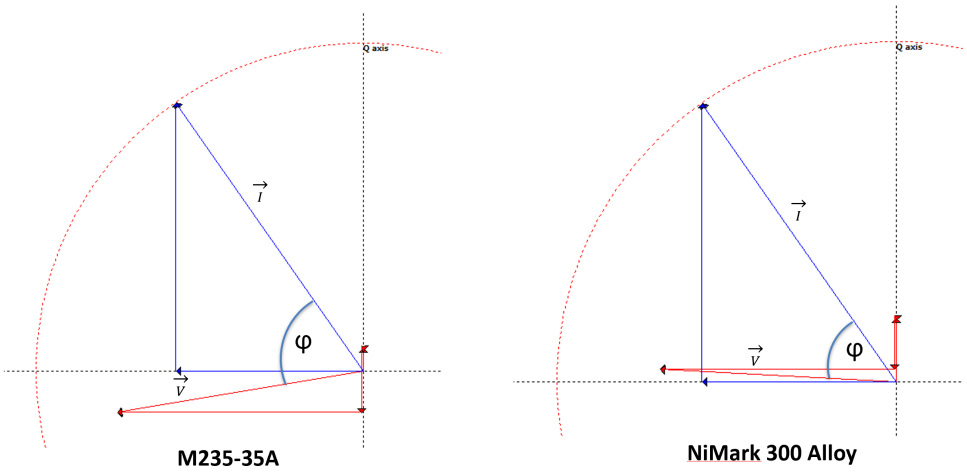

Figure 3.8: Phasor diagram created by MotorCad

CHAPTER 4

CONCLUSION

Achieving a performance improvement through rotor structure adjustment is not an easy task nowadays, as most of the electric machines are operating at over 97% efficiency. In this thesis we managed to improve that by changing the material properties and pushing our rotor design to its limits. Thus, we can finally say that this research has been successful and therefore useful for the upcoming industry.

The first and most important conclusion we obtained from this thesis is that the material exchange indeed performs our machine but not as good as we expected. With a new material, we obtained a max. torque value of 29.8 Nm whereas with the common used material, we obtained 26.7 Nm, under same conditions. Although we can define this result as an improvement, we cannot say that it is a breakthrough in electric machines.
As we said in the last paragraph in (3.2.2), we also came to the conclusion that the core bridge reduction had a positive impact in the back emf created by the magnets. This could be an important side effect on electric machines, since it could be also used for PMSM, where the bridge size between the magnets is also taken into consideration.

After doing all the simulation in MotorCad under the explained conditions in section (3.2.1), we also wanted to observe how the increase of our armature current could affect on our overall performance. Thus, we decided to run our simulation at 1.5 its rated current (135 A) and after analyzing the results, we obtain a difference of almost 11 Nm between both designs. Hence, we also conclude that by an increase of the armature current, the torque difference between both designs raises with it.
On the other hand, we are some issues we encountered by doing this research that are important to mention. Firstly, this proposed change of material is

only suitable for high speed applications, due to the poor magnetic properties of our material under low power conditions. Secondly, we since the material was donated to our department, we do not have any information on the NiMark 300 Alloy price. Thus, it would be interesting to have a look at its price on the market and take this factor into consideration to decide if this material is really cost-effective.

Finally, we conclude our thesis by looking further to manufacture our designs. We demonstrated with simulations that this idea could work, but we will not know for sure until we are able to test it in real conditions and with actual materials. As we said in the introduction of this research, our goal was to manufacture our designs the spring semester of 2020, but due to the pandemic spreading all over the world, we will have to wait until everything calms down again.

REFERENCES

[1] G. Pellegrino, T. M. Jahns, N. Bianchi, W. L. Soong, and F. Cupertino, *The Rediscovery of Synchronous Reluctance and Ferrite Permanent Magnet Motors*. Padova, ITA: Springer, 2016.

[2] C. Li, D. Xu, and G. Wang, "High efficiency remanufacturing of induction motors with interior permanent-magnet rotors and synchronous-reluctance rotors," in *2017 IEEE Transportation Electrification Conference and Expo, Asia-Pacific (ITEC Asia-Pacific)*, 2017, pp. 1–6.

[3] G. Sieklucki, "An investigation into the induction motor of tesla model s vehicle," June 2018, pp. 1–6.

[4] C. McLeod, "10 top countries for rare earth metal production," March 2019, webpage. [Online]. Available: https://investingnews.com/daily/resource-investing/critical-metals-investing/rare-earth-investing/rare-earth-producing-countries/

[5] Z. Zhang, G. Li, Z. Qian, Q. Ye, and Y. Xia, "Research on effect of temperature on performance and temperature compensation of interior permanent magnet motor," in *2016 IEEE 11th Conference on Industrial Electronics and Applications (ICIEA)*, 2016, pp. 411–414.

[6] M. Ibrahim, E. E. Rashad, and P. Sergeant, "Performance comparison of conventional synchronous reluctance machines and pm-assisted types with combined star–delta winding," *Energies*, vol. 10, p. 1500, 09 2017.

[7] S. Musuroi, C. Sorandaru, M. Greconici, V. N. Olarescu, and M. Weinman, "Low-cost ferrite permanent magnet assisted synchronous reluctance rotor an alternative solution for rare earth permanent magnet synchronous motors," in *IECON 2013 - 39th Annual Conference of the IEEE Industrial Electronics Society*, 2013, pp. 2966–2970.

[8] P. Li, W. Ding, and G. Liu, "Sensitivity analysis and design of a high performance permanent-magnet-assisted synchronous reluctance motor for ev application," in *2018 IEEE Transportation Electrification Conference and Expo (ITEC)*, 2018, pp. 406–411.

[9] W. Zhao, H. Shen, T. A. Lipo, and X. Wang, "A new hybrid permanent magnet synchronous reluctance machine with axially sandwiched magnets for performance improvement," *IEEE Transactions on Energy Conversion*, vol. 33, no. 4, pp. 2018–2029, 2018.

[10] "Electrical steel," November 2019. [Online]. Available: https://en.wikipedia.org/wiki/Electrical-steel

[11] T. Mohri, Y. Chen, M. Kohyama, S. Ogata, A. Saengdeejing, S. Bhattacharya, M. Wakeda, S. Shinzato, and H. Kimizuka, "Mechanical properties of fe-rich si alloy from hamiltonian," *npj Computational Materials*, vol. 3, 12 2017.

[12] "Density of steel," 2020. [Online]. Available: https://amesweb.info/Materials/Density-of-Steel.aspx

[13] "The IEEE website," 2002. [Online]. Available: http://www.ieee.org/

[13]